

## Study of Strain and Structural Peculiarities in Different Stages of Two- and Three-High Screw Rolling

M. M. Skripalenko<sup>a,\*</sup>, B. A. Romantsev<sup>a</sup>, S. P. Galkin<sup>a</sup>, L. M. Kaputkina<sup>a</sup>, and M. N. Skripalenko<sup>a</sup>

<sup>a</sup>National University of Science and Technology MISiS, Moscow, 119049 Russia

\*e-mail: mms@misis.ru

Received March 1, 2019

**Abstract**—This study includes the screw rolling of several blank parts of 12Kh18N10T steel on a two- and a three-roll mill, followed by modeling test rollings in the DEFORM FEM software. The test rolling results were used to evaluate changes in the dispersion of average grain size and hardness in the nonstationary and stationary phases of screw rolling. The computer-aided modeling results were used to evaluate variations in strain effective. The studies allowed identifying the changes in the average grain size and hardness in the different rolling phases and defined the compliance with the kind of changes in the average grain size, hardness, and strain effective across the blank part volume. The computer-aided modeling and test evaluation showed the differences in the kind of strain effective variations in the nonstationary phase at two- and three-high rolling.

**Keywords:** screw rolling, grain size, hardness, strain effective, nonstationary rolling, stationary rolling

**DOI:** 10.3103/S0967091219100139

Screw rolling is used to produce seamless pipes, round blanks, bars, and hollow billets (shells). Radial-displacement rolling, i.e., screw rolling with increased feed and roll toe angles [1, 2] allows heavily refining the grain [3, 4] by enhancing the plasticity and strength [5, 6]. Due to enhanced material properties, screw rolling is applied for the deformation processing of steels [1, 2] and titanium and magnesium alloys [4]. Screw rolling processes have an extremely complex moldability pattern; it is very difficult to study them by experiment, especially in terms of analyzing stress-strain state (SSS) parameters. As a rule, the workability of blank parts in screw rolling is restricted by the generation of axial [8] or annular metal fracture [9, 10]. The common opinion on the causes of deformable metal destruction [11, 12] is yet to be elaborated. Screw rolling processes are broadly studied by computer-aided modeling in FEM software that allows predicting the fracture at screw rolling to a certain degree of accuracy [8, 11]. The search in abstract databases has not helped find any studies with the experimentally confirmed kind of distribution of SSS parameters in a particular screw-rolling pattern. The results of papers [1–4] allow partially revealing the connection between the kind of grain size variations and the strain effective; however, this is true only for the steady-state, stationary phase of three-high screw rolling [1, 2, 9]. The fracture at screw rolling is known to begin in the nonstationary phase [8, 11, 12]. The distribution of SSS parameters in the nonstationary phases of two and three-high rolling and the difference in the way these parameters are distributed has been shown by the team of authors of paper [13] on the basis

of computer-aided modeling, although without any experimental confirmation. Studying the phases of screw rolling on two- and three-roll mills for defining changes in strain and structural parameters by test evaluation and computer-aided modeling is a topical task.

This paper is aimed at carrying out test rollings of 12KH18N10T steel blank parts on a two- and three-roll screw rolling mill and using computer-aided modeling of test rollings to find out the differences in changes in grain size, hardness, and strain effective in the nonstationary and stationary phase, as well as comparing the CAM and test rolling results. The grain size was measured on transversal and longitudinal (axial) metallographic samples.

### EXPERIMENTAL TECHNIQUES

The influence of the screw-rolling pattern on the formation of the grain structure and the hardness of the fabricated blank parts were measured on a two- and three-roll mill by test rollings of 12KH18N10T austenitic steel blank parts with the following composition in wt %:  $\leq 0.12$  C;  $\leq 0.8$  Si;  $\leq 2$  Mn; 9 to 11 Ni;  $\leq 0.02$  S;  $\leq 0.035$  P; 17 to 19 Cr;  $\leq 0.3$  Cu; 0.4 to 1 Ti; 67 Fe. The original blank parts and the nondeformable witness specimen of 60 mm in diameter and 200 mm in length were made by longitudinal rolling. The original blank parts were heated up to 1150°C and cured for two hours before rolling. The blank part diameter after two- and three-high rolling was 54 and 52 mm, respectively. All the blank parts were water-cooled after rolling. The two-high rolling was carried out on

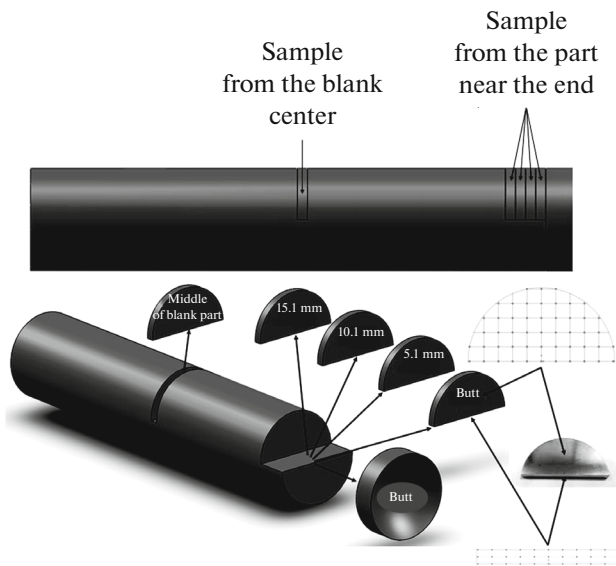


**Fig. 1.** Cutup sketch and arrangement of regions (points) for hardness and grain size measurements.

the MISiS-130D screw rolling mill with guide rulers and feed and rolling angles of 18 and zero degrees, respectively [10, 11, 14], and the three-high rolling—on the MISiS-100T [10] screw-rolling mill with feed and rolling angles of 18 and 10 degrees, respectively. The roll-rotation frequency was 55 1/min. Figure 1 shows how the specimens for the hardness and grain-size measurements were cut out.

The unsteady rolling phase was tested on specimens of 5 mm in thickness cut out from the part near the butt end with a cutting width of 0.1 mm. The steady phase corresponds to a similar half-round specimen cut out from the center of each blank part. A metallographic sample with the plane coincident with the blank part's axial section and a metallographic sample with the plane coincident with the blank part's cross section were made for each specimen. The way the grain size was measured in each of the cross samples in certain points is shown in Fig. 1: the points were located five mm from each other vertically and horizontally. The indicated grain sizes or hardnesses for each region are the average values found from 250 and three measurements, respectively, in a region of 1.3 mm<sup>2</sup> in area (1 × 1.32 mm rectangle). The results of the measurements in the points of the specimens from the region near the butt-end region were used to find the data in four cross sections and the data for twelve lines (diameters) in the longitudinal section (accordingly, each specimen from the region near the butt end had three longitudinal lines at 2.5 mm from each other) (See Fig. 1). It was taken that the cross section and the first of the three longitudinal lines of the specimen that became extreme after clipping the shrinkage cavity corresponded to the butt end; the distances for the rest of the cross sections and longitudinal section lines were calculated in millimeters from the butt end.

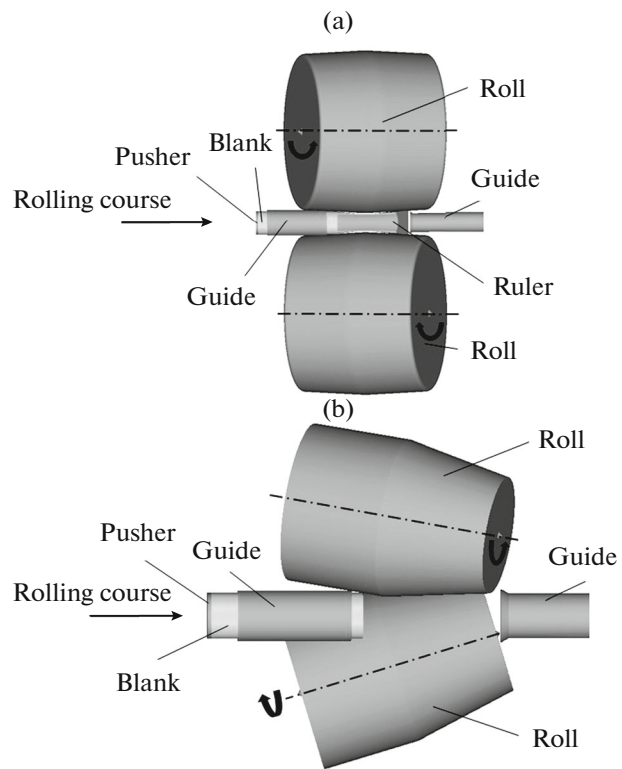


**Fig. 2.** Assemblies loaded to the DEFORM processor for modeling two- (a) and three-high (b) screw rolling, with the roll rotation and rolling directions indicated.

The surges in the samplings of data on average grain size and hardness were removed by Tukey's test [15] based on calculating the interquartile distance.

The microstructure was photographed by means of Axio Scope A1 Carl Zeiss and Axio Observer D1m Carl Zeiss microscopes using the Thixomet software [16]. The Vickers hardness number ( $HV_3$ ) was measured using an UH250 REICHERTER hardness meter. The surface of the metallographic samples was exposed to anode etching in 10-% of oxalic acid ( $C_2H_2O_4$ ) in water.

#### Computer-Aided Modeling Procedure

The test rollings were modeled in the DEFORM FEM software. First, however, assemblies of rolls, rulers, guides, a pusher and a blank part were created in the SolidWorks suite, saved as .stl files, and only then loaded to the DEFORM preprocessor. Figure 2 shows the assemblies loaded in the DEFORM preprocessor and the axes and rotation directions of the rolls and rolling. The third roll is not shown in Fig. 2b for convenience. After the assemblies were loaded to the preprocessor, the initial and boundary conditions were set according to the test rollings data. The modeling was carried out without considering the heat exchange between the blank part and the rolls, as well as the rul-

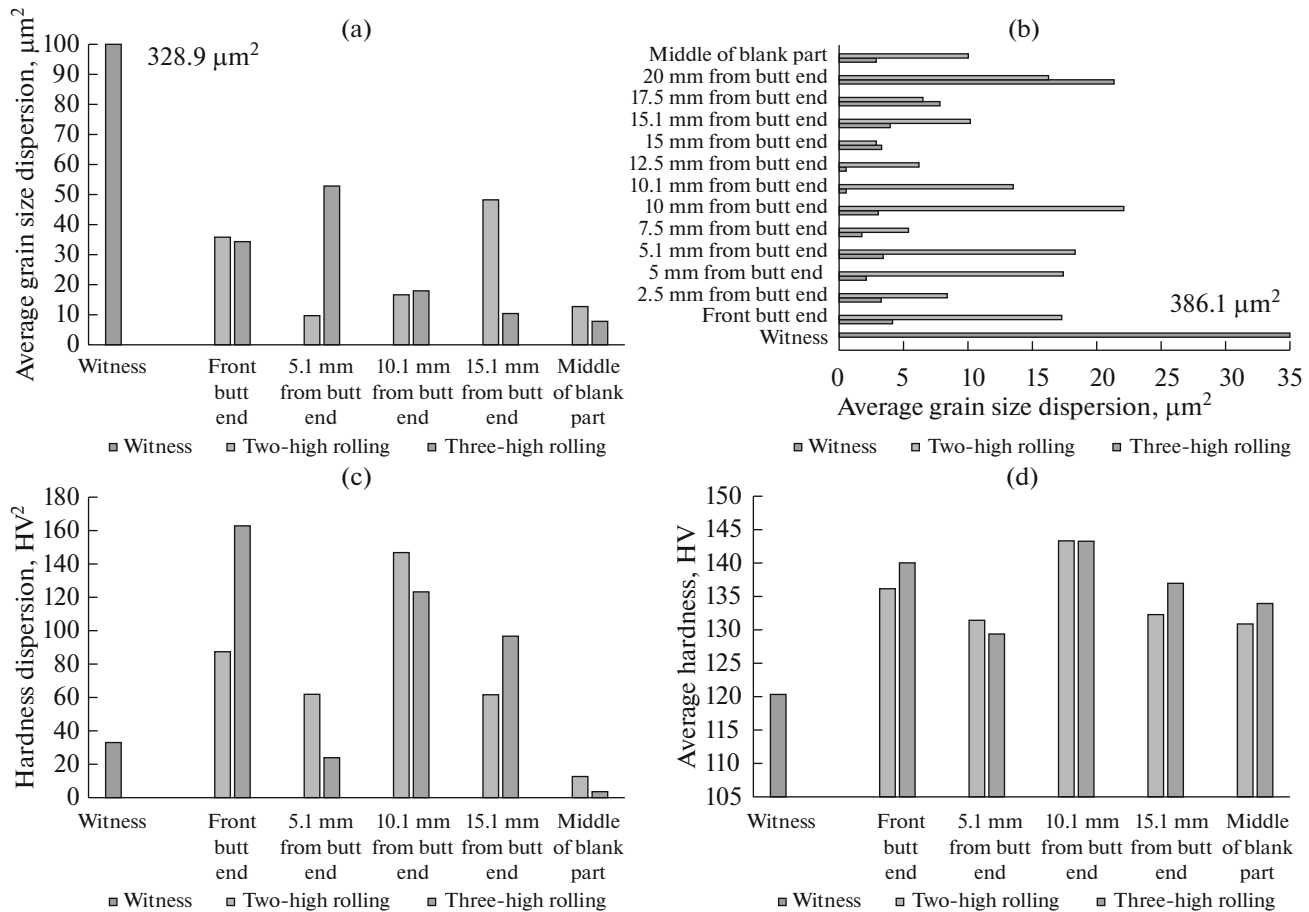


**Fig. 3.** Longitudinal (a) and cross section (b) distribution dispersion of average grain size; distribution dispersion of hardness values (c) and average hardness values (d) in cross sections at two- and three-roll rolling.

ers, guides, and pusher. The blank part had a lattice of 100000 tetrahedral finite elements; the Sybel friction factor for roll-blank, ruler-blank, pusher-blank, and guide-blank pairs was set equal to one, 0.3, 0.3, and 0.12, respectively. The blank parts were made from AISI-321 steel with a chemical composition in wt % similar to the one of the tested steel:  $\leq 0.08$  C;  $\leq 2$  Mn;  $\leq 0.045$  P;  $\leq 0.03$  S;  $\leq 0.75$  Si; 17 to 19 Cr; 9 to 12 Ni;  $\leq 0.01$  N;  $\leq 0.7$  Ti.

## RESULTS AND DISCUSSION

The calculated parameters were the cross and longitudinal section distribution dispersion of average grain size and the distribution dispersion of hardness values and average hardnesses after the rolling on the two- and three-roll mill (Fig. 3).

According to the data from Figs. 3a and 3b, the cross and longitudinal section dispersion in grain size at two- and three-high rolling are, respectively, 34, 133, 42, and 700 times as weak as those of the witness specimen. However, it should be noted that the screw rolling has a comparatively weak crimp: 10% for two- and 13% for three-high rolling. The essentially similar

results for the reduction in grain size at three-high screw rolling are presented in papers [3–7, 12], whereas no such studies have been found for two-high screw rolling.

In the nonstationary phase, the cross sectional dispersion of hardness (Fig. 3c) at two- and three-high rolling increases, respectively, by up to 390 and 400% as compared with the unstrained blank part. However, in the stationary phase, the dispersion of hardness weakened by 160 and 820% at two- and three-high rolling, respectively. The average cross sectional hardnesses (Fig. 3d) are higher than in the unstrained blank part: in the nonstationary phase, the increase was up to 20% for both rollings, and in the stationary phase the increase was 8% at two-high and 11% at three-high rolling.

The analysis of Fig. 3 has allowed finding out how grain size and hardness change in the nonstationary and stationary phase of both rollings. In the stationary phase, the spread of values for both rolling patterns is close to or narrower than in the nonstationary phase: in the stationary and nonstationary phase, the cross sectional distribution dispersion of average grain size for two- and three-high rolling is 12.71, 9.71 to 48.23,

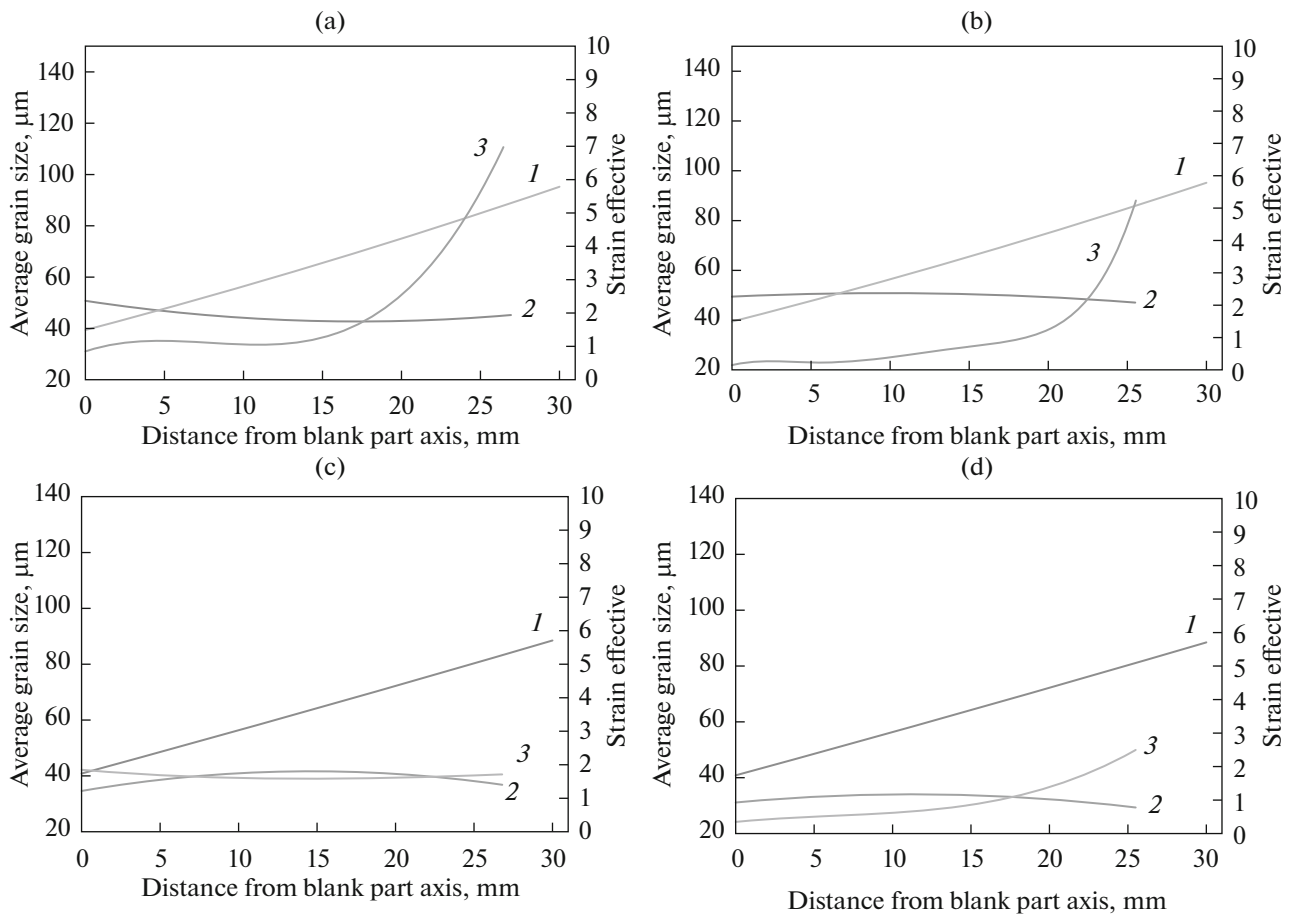


**Fig. 4.** Changes in strain effective radius (3) and grain size before (1) and after (2) two- (a, c) and three-high (b, d) rolling in cross section in the nonstationary and stationary phases, respectively.

7.82, and 10.41 to 52.85 sq.  $\mu\text{m}$ , respectively; the longitudinal section distribution dispersion of average grain size for two- and three-high rolling is 10.30, 2.89 to 22.1, 2.88, and 0.55 to 21.35 sq.  $\mu\text{m}$ , respectively. In the stationary phase, the spread of hardness values for both rolling patterns is narrower than in the nonstationary phase: in the stationary and nonstationary phase, the cross-sectional distribution dispersion of hardness for two- and three-high rolling is 12.65, 61.93 to 146.81, 3.59 and 23.93 to 162.83  $HV_5$ , respectively. In the stationary phase, the average cross-sectional hardness values in  $HV$  are closer than in the nonstationary phase: 130.8 and 131.43 to 143.32 for the two-high and 133.94 and 129.38 to 143.26 for the three-high rolling, respectively. The foregoing information allows assuming that in the stationary phase the properties are distributed across the blank part volume more evenly than in the nonstationary phase. The majority of publications about studying the screw-rolling influence on the properties of strained materials evaluate their change only in the stationary phase [4–6]. There are recommendations on clipping butt end regions in items produced by screw rolling, i.e., deformable in the nonstationary phase. The fulfilling

of these recommendations may cause significant losses in metal. Because of the potential difference in the properties of metal at stationary and nonstationary two- and three-high rolling in this paper, as well as in paper [17] for three-high rolling, it seems a relevant solution to control the moldability and, therefore, properties of metal at nonstationary rolling with the help of profiled blank parts like it is suggested, for example, in papers [18, 19].

The increase in hardness at three-high rolling, which is shown in Fig. 3D, has already been observed earlier, for example, in papers [3–7]. The published sources appear to contain no similar information for two-high screw rolling.

The test rolling and computer-aided modeling results have allowed identifying the connection between the kind of changes in grain size and the strain effective. It has been established that the reduction in grain size near the surface of an unstrained witness specimen is up to four times higher than in the specimen center. This implies that the strain near the blank-part surface is much more intensive than in the blank-part center. The indicated assumption is confirmed in Fig. 4 for the cross section found 15.1 mm away from

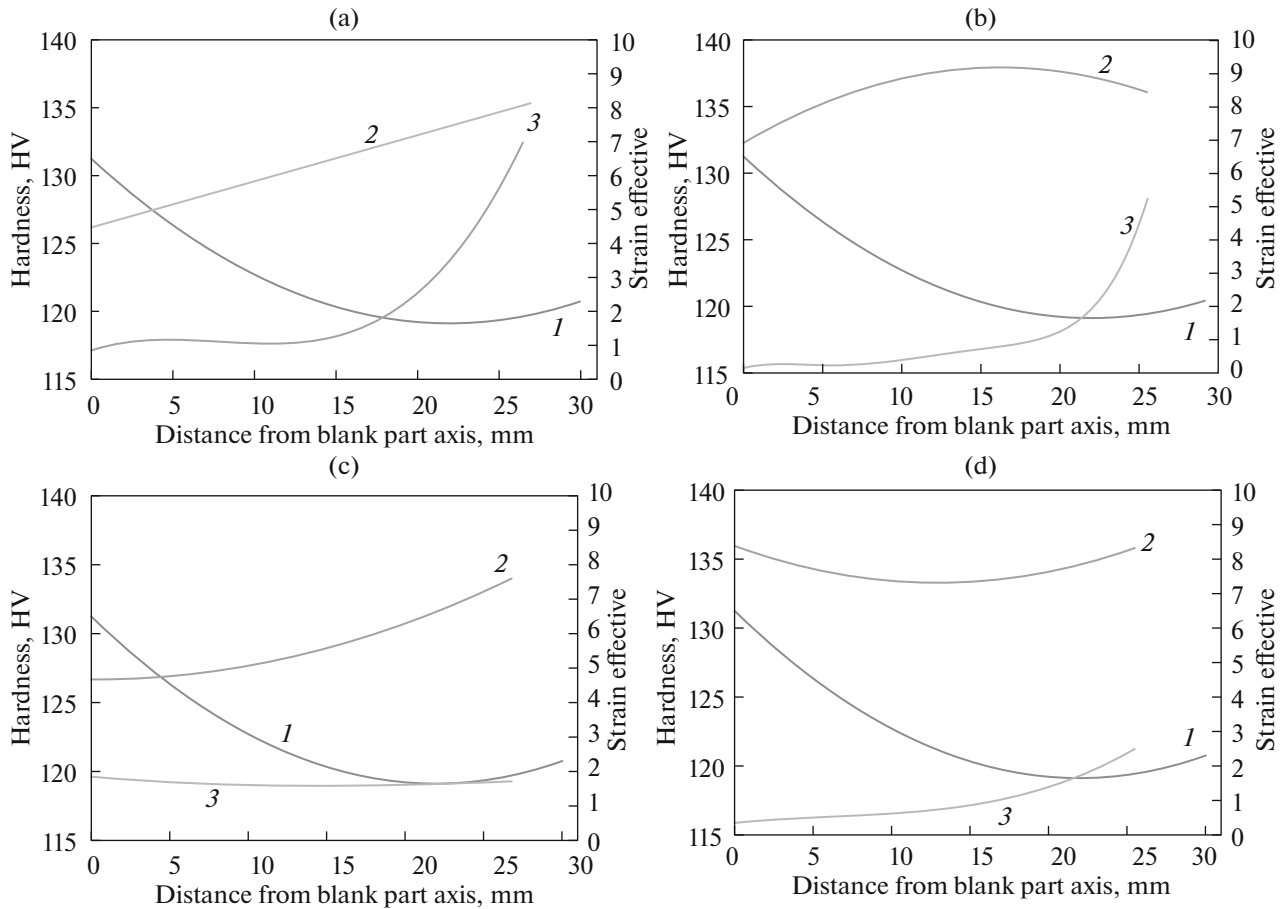


**Fig. 5.** Changes in strain effective radius ( $\beta$ ) and hardness before ( $I$ ) and after ( $2$ ) two- (a, c) and three-high (b, d) rolling in cross section in the nonstationary and stationary phases, respectively.

the butt end (nonstationary phase) and in the cross section in the blank-part center.

The changes in the cross-sectional hardness and strain effective (Fig. 5) were evaluated in the nonstationary and stationary phase in the manner similar to the one in Fig. 4. The hardness of the blank part surface increases much more significantly than the blank-part center hardness and then the hardness of the part blank heated and cooled without strain.

According to Figs. 4 and 5, the spread in strain intensities at two-high rolling in the stationary phase is twelve and 2.4 times narrower than in the nonstationary phase. The reduction in the spread of strain intensities largely explains the fact that in the stationary phase the distribution dispersion of hardness and average grain size is less significant than in the nonstationary phase (see Fig. 3).

The analysis of changes in grain size at screw rolling is of value not only in predicting the properties of produced items but also for understanding the essence of screw rolling. As defined by the authors of [13, 20] during computer-aided modeling without experimental confirmation, the nonstationary phase of two- and

three-high screw rolling is characterized by the W- and U-shaped longitudinal section distribution of strain effective (Fig. 6).

The changes in strain effective similar to those shown in Fig. 6 were obtained according to the results of computer-aided modeling of test rollings in DEFORM (Fig. 7). If drawing the blank part radius (the dashed line in Fig. 7), one of the isolines for two-high rolling will be crossed twice (isoline  $J$ ), whereas at three-high rolling each isoline is crossed only once. At two-high rolling, the radial strain effective decreases and then increases, whereas at three-high rolling it only increases. Considering the trend mapped in Fig. 5 and according to the radii indicated in Fig. 7a, the grain size at two-high rolling must first increase and then decrease, whereas at three-high rolling this size only decreases. This is confirmed by Fig. 7b. The correlation coefficients found using the data, that reflect the changes in grain size and strain effective, are  $-0.80$  and  $-0.89$  for two- and three-high rolling, respectively, and confirm the reverse correlation dependence.

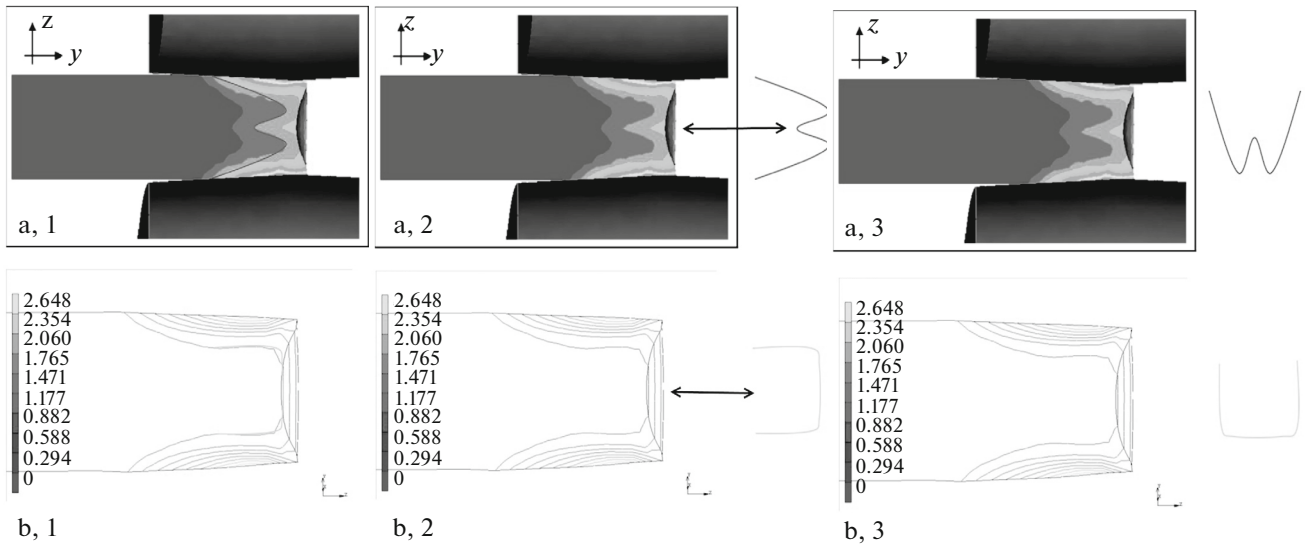


**Fig. 6.** Longitudinal section changes in strain effective in the nonstationary phase of two- (a) [20] and three-high (b) [13] screw rolling.

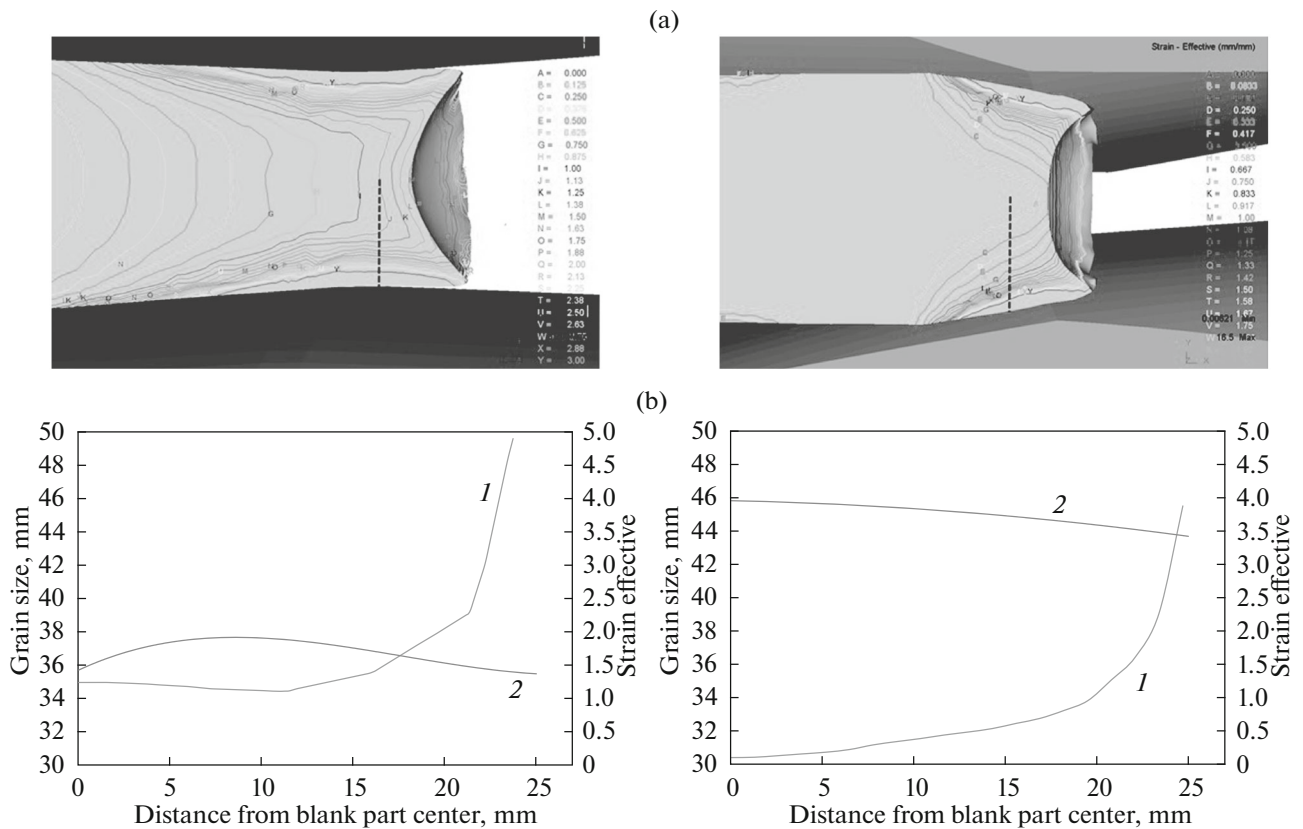


**Fig. 7.** Strain effective fields (a) and variations in strain effective (*I*) and average grain size (*2*) by radius in longitudinal section (b) in the nonstationary phase of two- (left) and three-high (right) screw rolling.

In addition to the results exposed in [11, 21, 22], the experimentally confirmed difference in the strain effective distribution in the nonstationary phase of two- and three-

high screw rolling proves the efficiency of applying test evaluation and computer-aided modeling to studying the SSS features of metal exposed to screw rolling.

## CONCLUSIONS

The screw rolling tests of 12Kh18N10T austenitic steel-blank parts on a two- and a three-roll mill and the computer-aided modeling of test rollings in the DEFORM FEW software have allowed attaining the following results:

In the stationary phase of two- and three-high rolling, the distribution dispersion of average in-section grain size is close to or lower than the similar distribution in the nonstationary phase; as to the unstrained blank part, however, the distribution dispersion of average grain size declines by ten folds.

The average hardness increases by 20% after both rollings, and the distribution dispersion of hardness across the rolled metal section in the nonstationary and stationary phase relative to the unstrained blank part increases by up to 400 and decreases by up to 800%, respectively.

The connection exists between the kind of changes in grain size and strain effective upon two- and three-high rolling.

The conjecture that the strain effective distribution field in the nonstationary phase is W-shaped at two-high and U-shaped at three-high rolling has been confirmed experimentally.

The spread of strain intensities in the stationary phase at two- and three-high rolling narrows by up to 1100 and 140% compared to the nonstationary phase, which can be the possible cause of the registered narrowing in the spread of hardness and average grain size values in the stationary phase of screw rolling relative to the nonstationary phase.

## REFERENCES

- Galkin, S.P., Romantsev, B.A., and Kharitonov, E.A., Implementation of the innovative potential of the universal method of radial-shear rolling, *Chern. Met.*, 2015, no. 1 (997), pp. 23–28.
- Galkin, S.P., Technology and mini-mills of radial-shear rolling as an optimal technique for creation of lean production, *Stal'*, 2014, no. 1, pp. 39–42.
- Li Wang, Y., Molotnikov, A., Diez, M., et al., Gradient structure produced by three roll planetary milling: numerical simulation and microstructural observations, *Mater. Sci. Eng., A*, 2015, vol. 639, pp. 165–172.
- Dobatkin, S., Galkin, S., Estrin, Y., et al., Grain refinement, texture, and mechanical properties of a magnetism alloy after radial-shear rolling, *J. Alloys Compd.*, 2018, vol. 774, pp. 969–979. <https://doi.org/10.1016/j.jallcom.2018.09.065>
- Stefanik, A., Szota, P., Mróz, S., et al., Properties of the AZ31 magnesium alloy round bars obtained in different rolling processes, *Arch. Metall. Mater.*, 2015, vol. 60, no. 4, pp. 3001–3006.
- Ratochka, I.V., Mishin, I.P., Lykova, O.N., et al., Structural evolution and mechanical properties of a VT22 titanium alloy under high-temperature deformation, *Russ. Phys. J.*, 2016, vol. 59, no. 3, pp. 397–402.
- Lopatin, N.V., Salishchev, G.A., and Galkin, S.P., Mathematical modeling of radial-shear rolling of the VT6 titanium alloy under conditions of formation of a globular structure, *Russ. J. Non-Ferrous Met.*, 2011, vol. 52, no. 5, pp. 442–447.
- Ghiotti, A., Fanini, S., Bruschi, S., and Bariani, P., Modeling of the Mannesmann effect, *CIRP Ann.*, 2009, vol. 58, no. 1, pp. 255–258.
- Teterin, P.K., *Teoriya poperechnoi i vintovoi prokatki* (Theory of Cross-Section and Helical Rolling), Moscow: Metallurgiya, 1983.
- Romantsev, B.A., Goncharuk, A.V., Vavilkin, N.M., and Samusev, S.V., *Trubnoe proizvodstvo* (Pipe Production), Moscow: Mosk. Inst. Stali Splavov, 2011.
- Skripalenko, M.M., Romantsev, B.A., Galkin, S.P., et al., Prediction of the fracture of metal in the process of screw rolling in a two-roll mill, *Metallurgist*, 2018, vol. 61, nos. 11–12, pp. 925–933.
- Nikulin, A.N., *Vintovaya prokatka. Napryazheniya i deformatsii* (Helical Rolling: Stresses and Deformations), Moscow: Metallurgizdat, 2015.
- Li, S.Z., Meng, W.H., Hu, L.W., and Ding, B., Research on the tendency of inner crack during 3-roll skew rolling process of round billets, *Adv. Mater. Res.*, 2011, vol. 145, pp. 238–242.
- Skripalenko, M.M., Bazhenov, V.E., Romantsev, B.A., et al., Mannesmann piercing of ingots by plugs of different shapes, *Mater. Sci. Technol.*, 2016, vol. 32, no. 16, pp. 1712–1720.
- Tukey, J.W., *Exploratory Data Analysis*, Reading, Mass.: Addison-Wesley, 1992.
- Expertise M., Thixomet: the system for microscope image analysis, laboratory. <https://thixomet.ru/>. Accessed September 23, 2018.
- Galkin, S.P., Theory and technology of stationary helical rolling of billets and bars of low-plastic steels and alloys, *Doctoral (Eng.) Dissertation*, Moscow: Moscow Inst. Steels Alloys, 1998.
- Karpov, B.V., Skripalenko, M.M., Galkin, S.P., et al., Studying the nonstationary stages of screw rolling of billets with profiled ends, *Metallurgist*, 2017, vol. 61, nos. 3–4, pp. 257–264.
- Karpov, B.V., Skripalenko, M.N., Skripalenko, M.M., et al., Modeling of the formation of sink mark during three-roll helical rolling on mini-mills, *Kuznechno-Shtampovochnoe Proizvod.—Obrab. Mater. Davleniem*, 2017, no. 1, pp. 19–26.
- [http://paduaresearch.cab.unipd.it/1552/1/Silvio\\_Fanini\\_Tesi\\_Dottorato.pdf](http://paduaresearch.cab.unipd.it/1552/1/Silvio_Fanini_Tesi_Dottorato.pdf). Accessed September 19, 2018.
- Skripalenko, M.M., Galkin, S.P., Her Jae Sung, et al., Prediction of potential fracturing during radial-shear rolling of continuously cast copper billets by means of computer simulation, *Metallurgist*, 2019, vol. 62, nos. 9–10, pp. 849–856.
- Naizabekov, A.B., Lezhnev, S.N., Arbuz, A.S., and Panin, E.A., Obtaining of long-length rods with ultrafine-grained structure by the radial-shear rolling, *IOP Conf. Ser.: Mater. Sci. Eng.*, 2018, vol. 461, pp. 1–5. <https://doi.org/10.1088/1757-899x/461/1/012065>

Translated by S. Kuznetsov